Experimental Characterization of the Solid Phase Chaotic Dynamic in Three-Phase Fluidization

ARTICLE *in* INTERNATIONAL JOURNAL OF MULTIPHASE FLOW · SEPTEMBER 1995

Impact Factor: 2.06 · DOI: 10.1021/ie00048a007

5 AUTHORS, INCLUDING:

Miryan C. Cassanello
University of Buenos Aires
67 PUBLICATIONS **581** CITATIONS
SEE PROFILE

Jamal Chaouki
Polytechnique Montréal
276 PUBLICATIONS **3,591** CITATIONS
SEE PROFILE

Experimental Characterization of the Solid Phase Chaotic Dynamics in Three-Phase Fluidization

Miryan Cassanello,† Faïçal Larachi, Marie-Noëlle Marie, Christophe Guy, and Jamal Chaouki*

Department of Chemical Engineering, École Polytechnique de Montréal, P.O. Box 6079, Station "Centre-Ville", Montréal, Québec, Canada, H3C 3A7

An experimental study of the solid phase dynamics in a three-phase fluidized bed reactor using heavy and light particles is carried out. A radioactive particle tracking technique is employed to obtain extended time series of the tracer path. The tracer has the same properties as the rest of the particles in the bed. A rescaled range analysis is applied to time series of the fluctuating velocities to investigate the features of solid phase turbulence. It is found that turbulence is anisotropic. In the axial direction, the correlations between the fluctuating velocities are persistent in time, indicating a superdispersive axial dispersion of the solids. Hence a constant axial dispersion coefficient, which is traditionally used in these reactors to represent the solid phase turbulence, only constitutes a lumped parameter hardly extrapolable to different operating conditions, different systems, and different geometries. The tracer path is also analyzed according to the theory of deterministic chaos. It is found that the solids motion is chaotic. An increase in the gas flow rate increases the values of the parameters that quantify the chaotic behavior of the solids motion. This analysis is found to constitute a promising tool to determine flow regime transitions.

Introduction

Gas–liquid–solid fluidized bed reactors are extensively used in the chemical, petrochemical, and biochemical industries. Development of accurate mathematical models for such reactors is still a challenge partially due to the complex and hardly understood dynamics of the fluidized particles. The solids motion is a resultant of interactions among the particles, with the fluid phases and the reactor walls, and is still poorly characterized (Wild and Poncin, 1993; Fan, 1989). Only a few works have studied the solids mixing of uniform particles in three-phase fluidized beds or sparged reactors (Bickel and Thomas, 1982; Euzen and Fortin, 1987; Khare et al., 1989; Fan et al., 1992; Tzeng et al., 1993). The last works have given a qualitative description of instantaneous solids patterns within wakes and vortices from video recording in a two-dimensional reactor. From them it became apparent that the solids dynamics is complex. Therefore, it is very important to achieve further fundamental insights in the solids motion in order to formulate precise hypotheses on their behavior for simulation or scale-up of three-phase fluidized bed reactors.

The solids motion is generally ensured by convection and dispersion. The dispersive characteristics of the particles motion can be determined from the analysis of their high-frequency fluctuations. In turbulent flow, such fluctuations are usually correlated and lead to "superdispersive" mechanisms, where the mean square fluctuating displacements scale with time as t^{α}, $\alpha > 1$. It has been shown (Wang and Lung, 1990) that certain dispersive mechanisms, in which the fluctuations are not Markovian, can be modeled by considering that the particles follow a fractional Brownian motion (FBM) as defined by Mandelbrot and Van Ness (1968). In a FBM, the fluctuating particles steps are correlated even for very long time. The magnitude of this correlation can be quantified by a rescaled range (R/S) statistical analysis. This analysis was first proposed by Hurst (1951) and modified and applied to FBM by Mandelbrot and Wallis (1969a).

A mean convective pattern of solids motion in three-phase fluidized bed reactors was evidenced by a radioactive particle tracking (RPT) technique and characterized by an Eulerian velocity map (Larachi et al., 1993). Notwithstanding, the qualitative information obtained by Tzeng et al. (1993) and some very high instantaneous velocities found with RPT indicate a solids dynamics much more complex than what is reflected in the mean patterns.

As was suggested by Stringer (1989) and only recently shown by Daw et al. (1990, 1991, 1992), Schouten and van den Bleek (1992), and van den Bleek and Schouten (1993a,b), the hydrodynamics of a gas–solid fluidized bed is chaotic. This was put into evidence from the analysis of pressure fluctuations and local voidage time series. Moreover, it was suggested that to account for the chaotic hydrodynamics would be of relevant importance in modeling and scale-up of gas fluidized beds (van den Bleek and Schouten, 1993a,b). The chaotic behavior may arise from the particles motion, and consequently it may also be a feature of the solids motion in three-phase fluidization.

A chaotic dynamics can be experimentally diagnosed by analyzing time series of a characteristic variable. The tools employed constitute the theory of deterministic chaos. This theory is a very fast growing field that proved to be applicable in many disciplines. Introductory references (Stewart, 1989; Ruelle, 1991) and comprehensive treatments specially written for engineers and applied scientists (Hilborn, 1994; Ott, 1993; Moon, 1992) are now available.

The purpose of this work is to experimentally study the qualitative characteristics of solids dispersion and convection in three-phase fluidized beds. Extended time series of positions of a solid tracer freely moving within

* Author to whom correspondence should be addressed. E-mail: jchaouki@mailsrv.polymtl.ca.

† Present address: PINMATE, Departamento de Industrias, FCEyN, Universidad de Buenos Aires, 1428 Ciudad Universitaria, Buenos Aires, Argentina.

0888-5885/95/2634-2971$09.00/0

the reactor are analyzed. The tracer mimics the solids constituting the fluidized bed, and its positions are obtained every 30 ms and for about 6 h by a noninvasive radioactive particle tracking technique (Larachi et al., 1994). The dispersive mechanisms of the solids motion are investigated through a *R/S* analysis of the time series. The correlations between the fluctuations are quantified, hence some features of the solids turbulence are obtained. Solids convection is characterized according to the theory of deterministic chaos. The Kolmogorov entropies are determined to certainly diagnose the existence of a chaotic dynamics. In addition, the dimensions of the attractor that describe the motion in a state space are estimated. The effect of a change in flow regimes on the magnitude of these parameters is studied.

Why Apply *R/S* Analysis and Deterministic Chaos Theory to Particle Tracking? A particle tracking technique provides the actual path of one of the solid particles in a multiparticle system. Assuming a hypothesis of ergodicity, this path would represent the motion of any equivalent particle at different instants if the tracking is long enough. Therefore, this technique allows the capture of the average dynamics of the solids motion since it gives instantaneous information sampled from all regions of the reactor.

The path of a solid particle in a turbulent medium is ensured by convection and dispersion. According to the statistical theory of turbulence, any step can be decomposed in a mean step plus a fluctuation. The convection is related to the mean steps while the fluctuations are responsible for the dispersion.

***R/S* Analysis Applied to the Fluctuating Steps.** The *R/S* analysis is a mathematical technique that aims at studying the fluctuating characteristics of a signal. Although it is usually employed as a pragmatic technique, when applied to the fluctuating steps of a moving particle, it gives quantitative information on the dispersive and diffusive features of the motion. As stated before, dispersion (diffusion on a molecular scale) arises from the fluctuating steps. For noncorrelated steps, the dispersion is Brownian like. Hence, it can be described by a Fickian law with a constant dispersion coefficient. If they are positively correlated, the dispersion is faster than in the Brownian case. This case is referred to as a superdispersive mechanism in which the variance of the steps does not have a linear time dependence. Consequently, the dispersion coefficient depends on time. On the contrary, for negatively correlated steps subdispersive mechanisms are encountered; the particles move slower than in the Brownian case, but the dispersion coefficient also depends on time.

If the particles also have a convective motion, the correlation between particle steps is not weak. A strong correlation is reflected in the *R/S* analysis. To get information on the dispersion in this case, the convective motion should be subtracted.

Finally, from a *R/S* analysis applied to particle fluctuating steps one can diagnose if a constant dispersion coefficient can be evaluated, compare the dispersive characteristics of turbulence for the different spatial coordinates to find out if turbulence is isotropic, search for differences in the solids dispersion characteristics for different flow regimes, and study the influence of introducing gas on the dispersive characteristics of liquid−solid fluidization.

Deterministic Chaos Theory. The time evolution (dynamics) of a multiparticle system can be obtained from a microscopic point of view by applying Newton's law to the motion of each particle. If the number of particles is high, the system is generally said to have infinite degrees of freedom. Until only a few years ago, it was thought that if one was able to write and compute the differential equations for all these degrees of freedom, the evolution of any system could be predicted. Nowadays it is known that there are systems in which the unpredictability is unavoidable since it arises from the sensitivity of the system evolution to the initial conditions (Moon, 1992; Hilborn, 1994). A differential uncertainty in the initial conditions grows exponentially in time and turns the system completely unpredictable even if it could be described by a few ordinary differential equations. Those systems are said to be chaotic.

The dynamics of a system is generally described in a state space. A point in this space represents the state of the system at a certain time. Its time evolution describes a trajectory. For a dissipative system, as time tends to infinity, the trajectory tends to a set of zero volume in the state space, an "attractor". Hence, an attractor describes the dynamics of a system after all transients have died out.

For the systems that are generally accounted for in chemical engineering, these attractors used to be fixed points or, for periodic evolutions, limit cycles; sets of dimension 0 or 1. When a system is chaotic, the attractors typically appear as very tangled geometrical objects usually with noninteger dimensions. They are known as fractal objects according to the definition of Mandelbrot (1982), and the attractors are called "strange attractors". The dimension of the attractor gives an indication of the degrees of freedom that remain active after all transients disappear.

Some advantages of applying deterministic chaos theory to the tracking of a particle in a multiparticle dispersed system, are summarized as follows: (1) It can be experimentally diagnosed if the particles motion shows chaotic behavior. This is essential to formulate and test mathematical models that pursue the microscopic description of this motion. A chaotic dynamics can only arise from a nonlinear description of its time evolution. Some qualitative and quantitative characteristics can be evaluated from the experimental data. This will allow the assessment of proposed models. In addition, the number of effective degrees of freedom that remain after the transients have died out can be obtained from the experimental data. (2) As the dynamics of the solids is strongly affected by the flow regime, it is highly probable that the parameters that quantify the chaotic behavior of the system will change with a change in the flow regime. This hypothesis, if verified by experimental data, constitutes an objective way to diagnose flow regime transitions in different systems.

Finally, it is possible that, for achieving a successful scaling of a reactor with a chaotic behavior, it might be necessary to perform an information balance. This hypothesis suggested by van den Bleek and Schouten (1993a) has to be experimentally confirmed from experiments in large scale reactors. These authors also suggested the definition of a dimensionless number that includes a quantitative chaos descriptor, the Kolmogorov entropy. For a proper scale-up, one should keep this number constant, together with the ordinary dimensionless numbers used to characterize the kinetics and transport phenomena.

Theoretical Concepts Applied

***R/S* Statistical Analysis.** *R/S* statistical analysis is a technique employed to characterize long-run correlations between apparently random fluctuations. A particle that moves with correlated fluctuating steps is said to have a fractional Brownian motion (FBM). This motion is characterized by a coefficient H, known as the Hurst coefficient. When $H = 1/2$, the process is Markovian with no correlation between the fluctuations. For $H > 1/2$, the correlation is positive, which indicates persistence and a superdispersive mechanism. For the case $H < 1/2$, the correlation is negative, suggesting antipersistence or subdispersion (Feder, 1988).

The *R/S* is defined as the ratio of the sample sequential range $R(t_0,s)$ of the FBM to the variance of the step lengths $S(t_0,s)$ for the time lag s, where:

$$R(t_0,s) = \max_{0 \le \eta \le s} c(t_0,s,\eta) - \min_{0 \le \eta \le s} c(t_0,s,\eta) \quad (1)$$

$$c(t_0,s,\eta) = [X(t_0+\eta) - X(t_0)] - \frac{\eta}{s}[X(t_0+s) - X(t_0)] \quad (2)$$

$$S(t_0,s) = \left\{\frac{1}{s}\sum_{\eta=t_0+1}^{\eta=t_0+s}[X(\eta) - X(\eta\text{-}1)]^2 - \left[\frac{1}{s}[X(t_0+s) - X(t_0)]\right]^2\right\}^{1/2} \quad (3)$$

and $X(t_0)$ is the position of the fractional Brownian particle at different initial instants. The rescaled range is a random function of the time lag s over which it is evaluated with the scaling property $R/S(s) \sim s^H$. Exponent H is directly estimated from the slope of $R/S(s)$ versus s in a log−log plot.

Chaotic Dynamics. Two of the most common parameters used to characterize strange attractors are its dimensions and the Kolmogorov entropy. In the following paragraph we give a brief description of how to reconstruct the attractor of a dynamical system from an experimental time series and definitions and methods for estimating the mentioned parameters.

Attractor Reconstruction. The qualitative dynamics of a dissipative system may be inferred from an experimentally obtained time series of a variable that provides information on the whole system. The attractor that describes the evolution of the system in state space may be reconstructed by generating vectors in an embedding state space from delayed measurements of one variable (Packard, 1980; Takens, 1981). These vectors can be expressed as

$$\underline{x}_t = \{v_t, v_{t+\tau}, v_{t+2\tau}, \ldots, v_{t+(m-1)\tau}\} \quad (4)$$

where v_t is the value of the measured variable at time t, τ is a delay time, and m is the dimension of the embedding space. Therefore, to obtain one point of the attractor in the embedding space, one should observe the chosen variable behavior for a window time of $m\tau$. The dimension of the embedding space should be large enough to avoid crossing of trajectories. Takens (1981) suggested $m > 2D + 1$, where D is the dimension of the minimum subspace containing the attractor.

For noisy experimental measurements, it is advisable to project the reconstructed attractor onto the components of a new basis of the embedding state space. In the new basis, the most significant components of the motion are more clearly observed. This may be carried out by the method of singular value decomposition (SVD) proposed by Broomhead and King (1986).

Attractor Dimension. A suitable quantity characterizing the attractor is its dimension. Actually, several dimensions are defined and they can be classified as "metric or fractal" dimensions and "probabilistic or natural measure" dimensions. The metric dimensions only consider the geometry of the attractor. The natural measure dimensions also provide a notion of the relative frequency with which a trajectory visits different regions of the attractor (Farmer et al., 1983). They typically take smaller values than the metric dimensions. Among the probabilistic dimensions, the "correlation dimension" is the simplest one to estimate from an experimental time series using a method proposed by Grassberger and Procaccia (1983a). The reason to evaluate the attractor dimension is that it provides an indication of the number of degrees of freedom of the dynamical system (i.e., the number of variables needed to describe the asymptotic state of the system).

The method uses the definition of the correlation integral:

$$C_\epsilon = \lim_{N\to\infty} \frac{1}{N^2}\sum_{i,j=1}^{N} \Theta(\epsilon - |\underline{x}_i - \underline{x}_j|) \quad (5)$$

where N is the number of data points in the reconstructed attractor and Θ is the Heaviside function, employed to count how many pairs of points $[\underline{x}_i, \underline{x}_j]$ in the state space are contained in a hypersphere of radius ϵ. The correlation dimension ν is evaluated from the scaling region of $\ln(C_\epsilon)$ vs $\ln(\epsilon)$. For a detailed description of this technique, Grassberger (1986) may be consulted.

An upper integer limit of the attractor dimension may be estimated from SVD. However, Albano et al. (1988) have shown that different dimensions would be determined depending on the pair (m,τ) employed for the embedding procedure. Hence, SVD is used to get clearer attractor representations but the dimensions are estimated by the method of Grassberger and Procaccia (1983a) corrected to account for the dynamical correlation (Theiler 1986, 1991).

Kolmogorov Entropy. An important characteristic of a chaotic system is its information loss rate; i.e., what is the required accuracy in the initial conditions to be able to predict the system evolution during a certain time period (Grassberger, 1986). The information loss in a chaotic system arises from the exponential divergence of very close trajectories. It is quantified by the Kolmogorov entropy. Positive values of the Kolmogorov entropy (KE) undoubtedly indicate chaotic evolutions.

For a dissipative nonchaotic system, the Kolmogorov entropy is nil. For a completely random process, its value is infinite, making it impossible to assess the state of the system even after a differential time step. For the case of a chaotic system, the KE is finite and positive (Grassberger and Procaccia, 1983b). A lower limit of the Kolmogorov entropy can be estimated by an algorithm suggested by Grassberger and Procaccia (1983b) that uses an extension of the definition of the correlation integral:

$$C_\epsilon^d = \lim_{N\to\infty} \frac{1}{N^2}\sum_{i,j=1}^{N} \Theta(\epsilon - [(\underline{x}_i - \underline{x}_j)^2 + (\underline{x}_{i+1} - \underline{x}_{j+1})^2 + \ldots + (x_{i+d} - x_{j+d})^2]^{1/2} \quad (6)$$

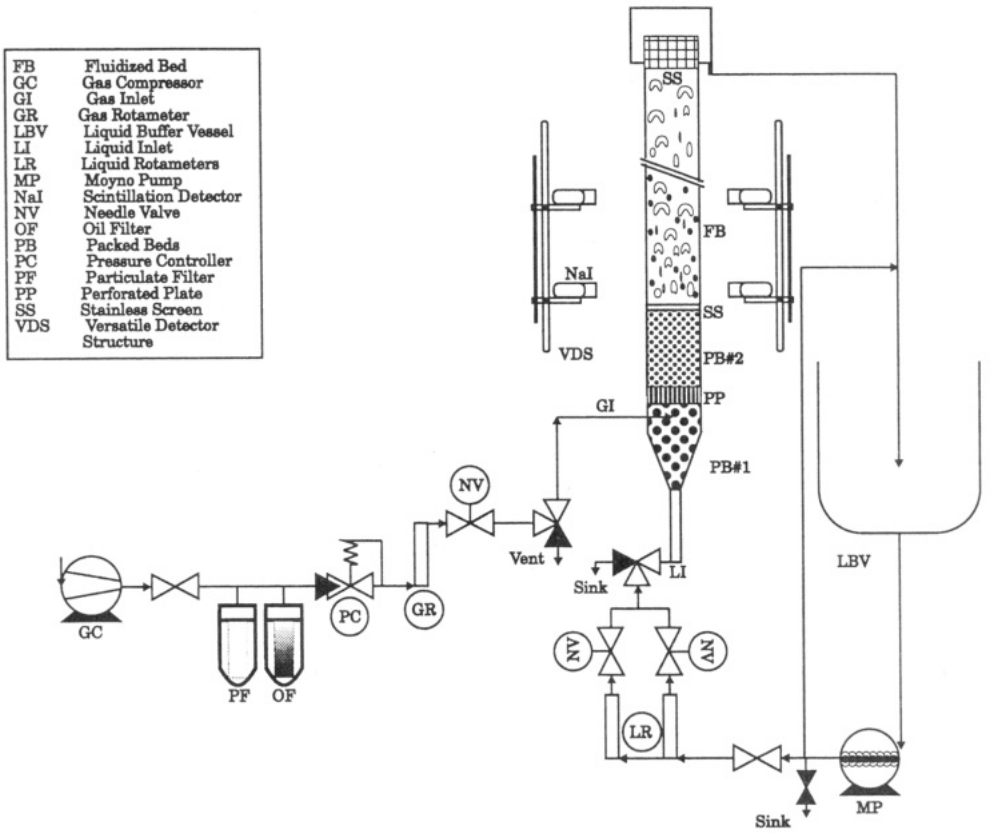

Figure 1. Schematic flow sheet of the experimental setup.

Experimental Section

The particle tracking technique had already proved its suitability to investigate the solid and liquid dynamics in gas–solid fluidized beds (Lin et al., 1985; Moslemian et al., 1989) and bubble columns (Duduković et al., 1991). The technique employed in the present work is built on these pioneering works and improved the capabilities of the particle tracking technique by including a model to account more accurately for the physics of the radiation phenomena (Larachi et al., 1994).

The experimental installation is schematically shown in Figure 1. It basically consists of an acrylic column, 0.1 m internal diameter and 1.5 m height. It has a 0.3 m high packed bed (glass beads of 2 mm) as the gas–liquid distributor, located above a 0.15 m high calming zone. The solids that were fluidized are 3 mm glass beads (ϱ_s = 2500 kg/m^3) or PVC particles (ϱ_s = 1320 kg/m^3) of 5.5 mm equivalent diameter. The latter were treated with sulfochromic solution to turn them wettable. The solids are fluidized in an air–water system. The total mass of solids used is 4 kg for glass beads and 0.8 kg for PVC particles. Bed heights at rest (no liquid flow) were, respectively, 0.35 and 0.2 m. Expanded bed heights were different for the different operating conditions and varied from 0.45 to 0.65 m.

The experiments carried out provide extended time series of positions of a solid radioactive tracer that represents the particles in the bed. The movement of the γ-emitting radioactive tracer, having the same properties as the solids constituting the fluidized bed, is continuously followed by an array of 8 NaI (Tl) scintillation detectors. Different amounts of γ-rays impinge on each detector depending on the tracer location in the bed and the corresponding subtended effective solid angle. The number of counts recorded also depends on the attenuation of the three-phase emulsion and the dead time of the detectors used. For each experiment, the counts accumulated by each detector for every 30 ms are recorded for about 6 h. Taking advantage of detector redundancy, the successive particle positions are calculated by inverse reconstruction algorithms. These algorithms are based on a phenomenological model that accounts for the mentioned variables, which determine the amount of radiation that reaches each detector. The statistical characteristics of the radiation are considered by Monte Carlo simulation. To accurately evaluate the attenuation in the bed, a calibration is performed for each experiment. The counts recorded by the detectors when the tracer is located at 150 known positions within the three-phase emulsion are measured. With these data, three parameters are optimized for each detector: the overall attenuation of the gas–liquid–solid emulsion, the detector dead time, and the source radioactivity. The uncertainty in the measurements is estimated from the calibration points and also by following a known trajectory in the emulsion. It was found that it is around 2 mm for the coordinates perpendicular to the net fluid flows and 6 mm for the axial coordinate. Further details on the technique and the experimental facility can be found in Larachi et al., 1994.

Experiments were carried out for liquid superficial velocities of 0.058 and 0.065 m/s. Gas superficial velocities were varied within the range $0 < u_G < 0.11$ m/s. Both homogeneous and heterogeneous flow regimes were observed in three-phase fluidization within these conditions. The change in flow regime when using the glass beads, as identified by visual inspection, corresponds to that predicted by Nacef (1991) (see also Wild and Poncin, 1993) for a static mixer distributor. This author employed glass beads similar to the ones used in this work to study flow regime transitions. For

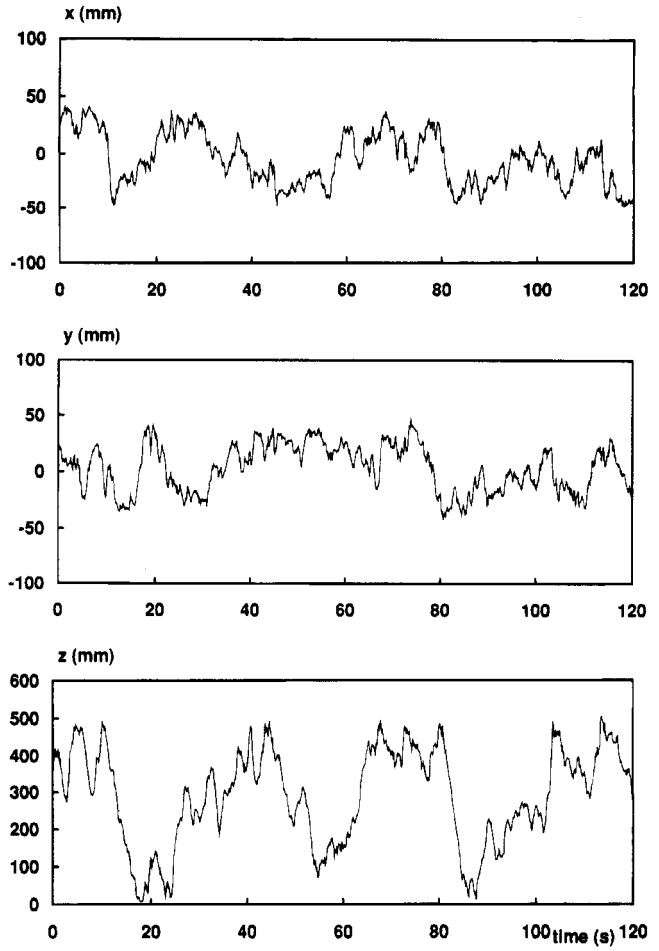

Figure 2. Time series of the tracer Cartesian coordinates for an experiment in the homogeneous flow regime. Fluidized particles: 3 mm glass beads; u_L = 0.065 m/s; u_G = 0.032 m/s.

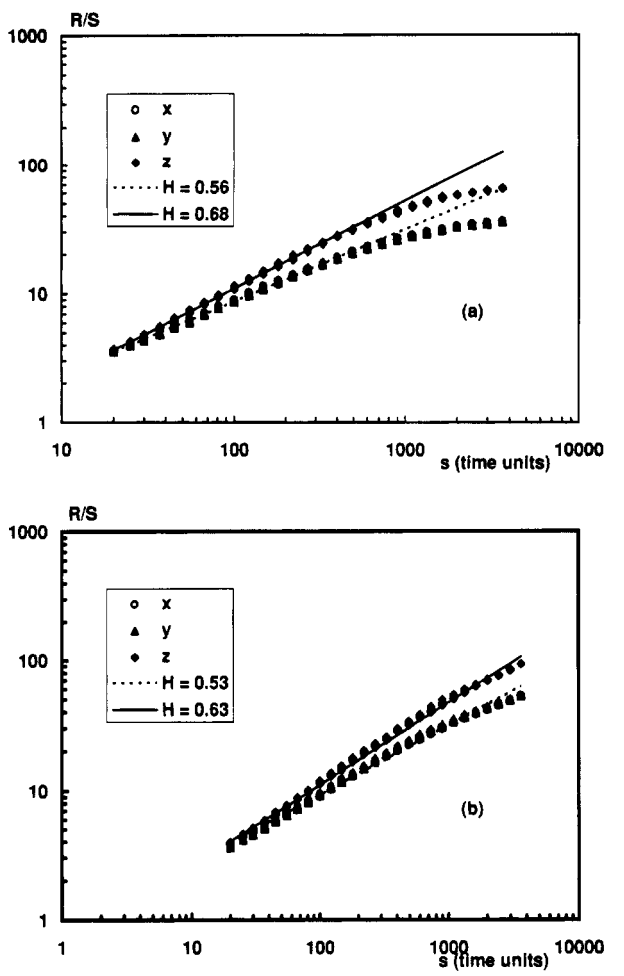

Figure 3. Pox diagrams for (a) the tracer Cartesian coordinates for the same experiment as in Figure 2 and (b) the fluctuating tracer steps for the experiment shown in Figure 2.

the light particles, we observed that onset of the heterogeneous flow regime appears at a lower gas velocity than the one predicted by Nacef (1991). For liquid–solid fluidization, the particulate flow regime was observed for the light particles and segregate flow regime for the glass beads.

Results and Discussion

***R/S* Statistical Analysis.** A representative period of the Cartesian coordinates of successive tracer positions for a gas–liquid–solid experiment is shown in Figure 2. Records of simulated FBM (see for example Feder, 1988) look similar to the obtained time series. Hence, as a first approximation, we applied the *R/S* analysis directly to the particle steps in order to examine if a FBM was able to account for the particle motion. To evaluate the rescaled ranges we considered different time lags s. We also employed a large number of initial times t_0 to obtain more representative estimations. The pox diagrams of the log(R/S) versus log(s) for the three Cartesian coordinates are shown in Figure 3a. The Hurst coefficients, H, are evaluated by least squares of the straight portion of the curves.

The following features are observed from the pox diagrams (Figure 3a): (1) the coordinates in the plane transverse to the net fluids flow (x,y) have completely similar behavior. In addition, the behavior is different from the axial one (z). This suggests an average axisymmetry and anisotropic motion of the solids in these reactors and (2) a deflection in the straight lines for large time lags s.

As was pointed out by Mandelbrot and Wallis (1969b), the presence of a break in the straight line in the pox diagram indicates deterministic components superimposed on the long-correlated random process under analysis. This suggests that the motion of solid particles in three-phase fluidization cannot be considered purely dispersive. There is also a strong convective component in the motion. Hence, time series of fluctuating velocities are calculated from the data by discounting the mean Lagrangian velocities from the instantaneous velocities. Mean Lagrangian velocities are calculated by discretizing the reactor and considering that every time the tracer crosses a certain compartment, a different trajectory is started there. The procedure is similar to the one used by Duduković et al. (1991). In this way, mean velocities corresponding to a small compartment in the reactor are evaluated by time averaging of instantaneous velocities. Then, the means are subtracted from the instantaneous velocities for the corresponding compartment to get time series of fluctuating velocities. A *R/S* is performed on these time series. The pox diagrams obtained for the same three-phase experiment are shown in Figure 3b. Even though a straightening of the curves is apparent, the difference for the axial behavior persists. Hurst exponents obtained for all operating conditions studied, after discounting the convective component, are listed in Table 1.

The estimated Hurst coefficients for the coordinates of the plane transverse to the net fluids flow are similar for the liquid–solid (u_G = 0) and gas–liquid–solid

Table 1. Calculated Hurst Exponents for Different Operating Conditions

solid	u_L (m/s)	u_G (m/s)	flow regime	H_x	H_y	H_z
glass beads	0.065	0	segregate	0.48 ± 0.02	0.48 ± 0.02	0.36 ± 0.02
d_p = 3mm	0.065	0.032	homogeneous	0.53 ± 0.02	0.52 ± 0.02	0.63 ± 0.02
ϱ_s = 2500 kg/m^3	0.065	0.069	transition	0.52 ± 0.02	0.49 ± 0.02	0.65 ± 0.02
	0.065	0.110	heterogeneous	0.44 ± 0.02	0.46 ± 0.02	0.68 ± 0.02
PVC particles	0.058	0	particulate	0.50 ± 0.02	0.48 ± 0.02	0.55 ± 0.02
d_p = 5.5 mm	0.058	0.010	homogeneous	0.49 ± 0.02	0.48 ± 0.02	0.57 ± 0.02
ϱ_s = 1300 kg/m^3	0.058	0.027	heterogeneous	0.48 ± 0.02	0.49 ± 0.02	0.63 ± 0.02

experiments. Hence, the dispersive motion of the solids in these directions is likely to be imposed mainly by the liquid motion and the interaction between the particles. The intensity of fluctuations probably increases by bubble−particle interactions in the case of three-phase fluidized beds, but the presence of gas does not change the transverse mixing mechanism.

For the axial direction, the Hurst coefficient is modified by the injection of gas. In the liquid−solid case, two different behaviors are observed: (1) for the segregated flow regime, the particles tend to stay in a preferential axial layer in the fluidized bed due to slight inhomogeneities in the size of the particles and the high solids holdup that induces strong particle−particle interactions. Therefore, the dispersion for this case is slower than for particles moving in Brownian way; hence Hurst exponent is lower than 0.5. This corresponds to an antipersistent FBM as was mentioned in the Introduction. (2) For the particulate flow regime, the Hurst exponent is slightly higher than 0.5, indicating a weak positive correlation that lasts in time.

For three-phase fluidization, Hurst exponents estimated for the axial direction for different experimental conditions slightly increase with gas velocity, which suggests that the type of flow regime does not significantly modify the axial dispersive process. As gas velocity increases, mean solid velocities are higher and the appearance of the break in the pox diagrams is more evident and occurs at lower time lags s. An increase in bubble coalescence may explain the increase in mean particle velocities. Bigger bubbles drift the solid particles more vigorously in their wakes. This effect increases the particles convection in the axial direction. Hurst coefficients for axial fluctuations are always different from 0.5, indicating that a Fickian law with a constant axial dispersion coefficient does not suitably represent the axial turbulent dispersion.

Yang et al. (1992) also applied a R/S to the fluctuating velocities of a liquid flow follower in bubble columns. For radial and axial coordinates, their results are similar to the ones obtained in this work for the solid in three-phase fluidization. However, they obtained a Hurst exponent of 0.7 for the azimuthal coordinate, indicating that a correlation of the fluctuations persists in time. This is probably due to the swirling motion of the bubbles that is more intense in a bubble column. Another interesting result observed by these authors is that the Hurst coefficients estimated for certain operating conditions are not very sensitive to a change in the column diameter. This suggests that boundary effects do not significantly affect the evaluation of the Hurst exponent from the fluctuating velocities.

Deterministic Chaos Theory. The motion of a solid tracer that freely moves within the reactor provides thorough information on the dynamics of the particles in three-phase fluidization. The motion of this tracer is the overall outcome of the effect of the different forces defining the evolution of the particles motion (i.e., particle weight, buoyancy, drift, and other interactions between the phases).

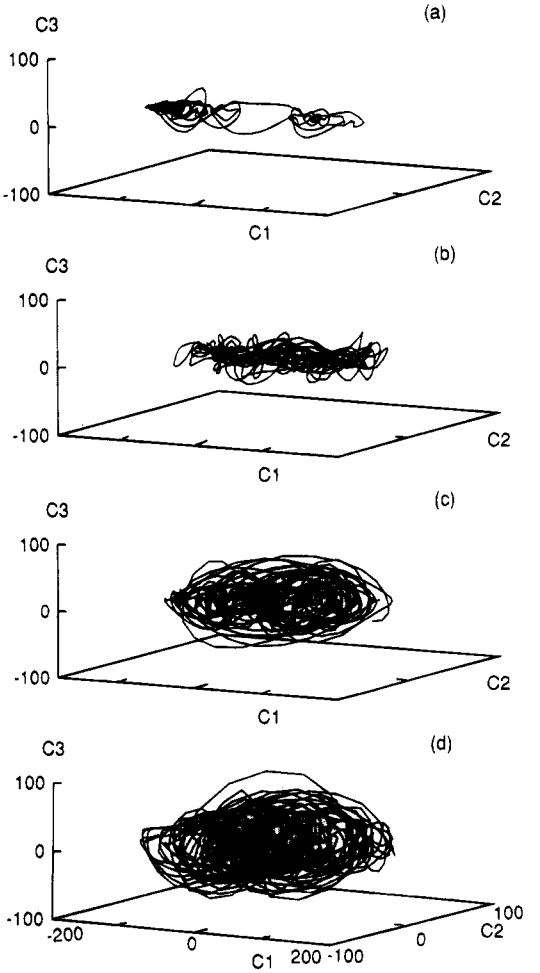

Figure 4. Reconstructed attractor projected in the first 3 principal eigenvectors obtained by SVD for different gas velocities. Solids: 3 mm glass beads; u_L = 0.065 m/s; (a) u_G = 0; (b) u_G = 0.032 m/s; (c) u_G = 0.069 m/s; (d) u_G = 0.110m/s.

Attractor Reconstruction. From the time series of any of the tracer coordinates, the attractor that qualitatively characterizes the particulate dynamics can be reconstructed following the embedding procedure described previously. The tracer positions are a resultant of a certainly deterministic motion induced by the complex interactions between the phases as was put into evidence in the last section. However, it also includes hydrodynamic fluctuations and a non-negligible noise introduced by the measuring technique. Hence the method of SVD (Broomhead and King, 1986) is applied. Projections of the reconstructed attractor from the x coordinate time series on the first three components of the new basis of the embedding state space are shown in Figure 4. The gas superficial velocity is the varying parameter for the different experiments. All figures are represented in the same scale for comparison. It is important to mention that by using different periods of data along the 6 h experiments, similar results are obtained for the reconstructed attractor and all the estimated parameters.

It is observed that the size of the attractor increases as the gas velocity increases. The trajectories for the gas–liquid–solid experiments are distributed more uniformly over the state space (Figure 4b–d) than for the liquid–solid case (Figure 4a). For liquid–solid fluidization, the majority of the trajectories are bounded in a small region in the state space. Only a few of them have longer excursions. This may indicate an attractor with very different features in different spatial positions. For three-phase fluidization, a strong difference is observed between the experiment carried out at the lower gas velocity (Figure 4b) and the two others. Interestingly, this change in the attractor shape corresponds to the appearance of large bubbles that could be observed through the reactor walls.

Attractor Dimensions. The correlation dimension was calculated using Grassberger–Procaccia's (1983a) algorithm. The points that are too close in time were not considered in the integral to account for the dynamical correlations (Theiler, 1986, 1991). Indeed, the curves of the correlation dimension versus ϵ exhibit a shoulder characteristic of the presence of dynamical correlation. Hence, the points too close in time were discarded to prevent the presence of the shoulder. Typically, the first 10 points were not considered. The correlation integral is evaluated for different embedding dimensions (starting from 5) and for different delay times (τ = 3–24 sample periods, increments of 3) with a relatively small number of data (10^4). Then, the combination (m,τ) that provides the widest plateau in the representation of (d ln(C_ϵ))/(d ln(ϵ)) versus ln (ϵ), is chosen, following the suggestion of Albano et al. (1988). A change in this combination often modifies the broadness of the plateau. However, if convergence is observed, it does not significantly change the value of the dimension. After the pair (m,τ) was chosen, the correlation dimension and the Kolmogorov entropy are recalculated with a larger number of points to get reliable estimations, starting from 2×10^4 and increasing this value if a change is observed from the results obtained with 10^4 points. Then, the convergence of the correlation dimension value is confirmed again with the larger number of data by representing the slope of ln(C_ϵ) versus ln(ϵ) for the chosen τ and different embedding dimensions (Figure 5).

The calculated correlation dimensions for the different operating conditions studied are listed in Table 2. The values of the correlation dimensions are low for liquid–solid fluidization. They suggest that the solid phase dynamics would be well described with only a few ordinary differential equations (Eckman and Ruelle, 1985). However, it should be noted that chaos theory does not provide information on which are the variables that completely describe the physical phenomena. For three-phase fluidization, the dimensions remain low at low gas velocities and increase strongly as large bubbles appear in the flow. The correlation dimension values for liquid–solid fluidization and three-phase fluidization with low gas velocities are similar to the ones found for the bubbling flow regime in gas–solid fluidized beds ($\nu \approx 4$) (van den Bleek and Schouten, 1993b).

Kolmogorov Entropy. The Kolmogorov entropy was estimated using the procedure suggested by Grassberger and Procaccia (1983b). The embedding dimension and delay time used for the correlation dimension estimation were employed. Similar plateaus were found for different numbers of consecutive points d, and the ratio of correlation integrals was taken in the range of sizes where the plateaus were overlapping.

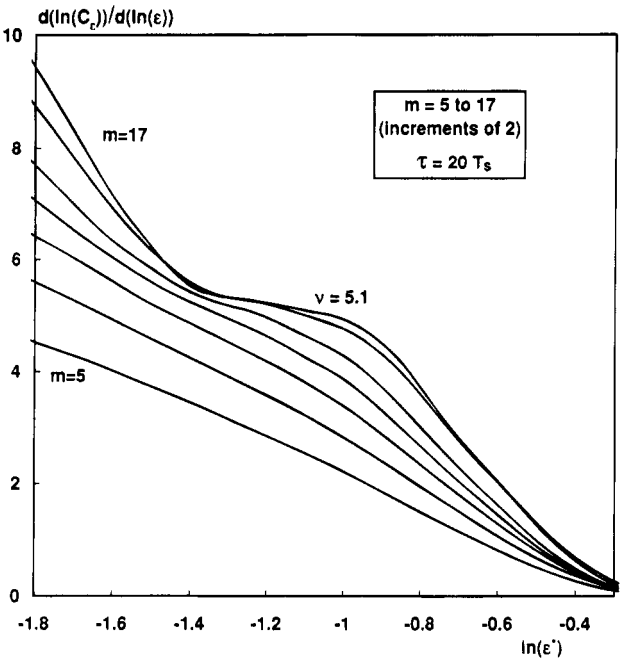

Figure 5. Convergence of the slope of ln(C_ϵ) vs ln(ϵ) for different embedding dimensions. Solids: 3mm glass beads; u_L = 0.065 m/s; u_G = 0.032 m/s.

A typical example of a Kolmogorov entropy calculation is shown in Figure 6 for a gas–liquid–solid experiment. Figure 6a shows the correlation integrals for different numbers of consecutive points. The resulting variation of the Kolmogorov entropy with d is presented in Figure 6b. The corresponding results are also listed in Table 2. The values are always positive, indicating that the particles dynamics is chaotic. The degree of chaotic behavior increases with an increase in gas velocity. This result indicates that a mathematical model aiming at representing the solids dynamics in three-phase fluidization should contain a minimum of nonlinear complexity since chaotic behavior can only arise from nonlinear equations. The chaotic characteristics should be reflected in the model as well as the effect of increasing the gas flow rate.

The influence of the gas superficial velocity on the Kolmogorov entropy and on the correlation dimension is shown in Figure 7a and b, respectively. As gas velocity is increased, large changes in the values of both parameters are observed, which are attributed to a change in flow regime. The gas velocities that correspond to a change from homogeneous to heterogeneous flow regimes as predicted from Nacef (1991) are also shown for comparison. As observed in the figure, the transition suggested by the analysis from the theory of deterministic chaos satisfactorily agree with Nacef's predictions which are based on visual observations. However, applying the theory of chaos to the path of a solid tracer has the advantage of being a criterion less subjective and more suitable for opaque systems. Moreover, this method examines the internal structure of the flow that cannot be observed by visual inspection through the reactor walls. The transition in flow regime appears to be gradual, especially for glass beads; however, it seems sharper for the light particles. More experiments are needed to confirm the trends.

The magnitude of the correlation dimension increases steadily with the gas superficial velocity, and no sharp

Table 2. Calculated Values for the Parameters Characterizing the Strange Attractor

solid particles	u_L (m/s)	u_G (m/s)	flow regime	ν	KE (bit/s)
glass beads	0.065	0	segregate	2.6	0.4
d_p = 3mm	0.065	0.032	homogeneous	5.1	0.9
ϱ_s = 2500 kg/m^3	0.065	0.069	transition	9.5	4.3
	0.065	0.110	heterogeneous	15.1	8.2
glass beads mixture 50% (w/w)	0.065	0.110	heterogeneous	13.1	12
d_p = 3 and 1 mm					
ϱ_s = 2500 kg/m^3					
PVC particles	0.058	0	particulate	3.3	0.6
d_p = 5.5 mm	0.058	0.010	homogeneous	3.5	0.6
ϱ_s = 1300 kg/m^3	0.058	0.027	transition	5.5	5.6

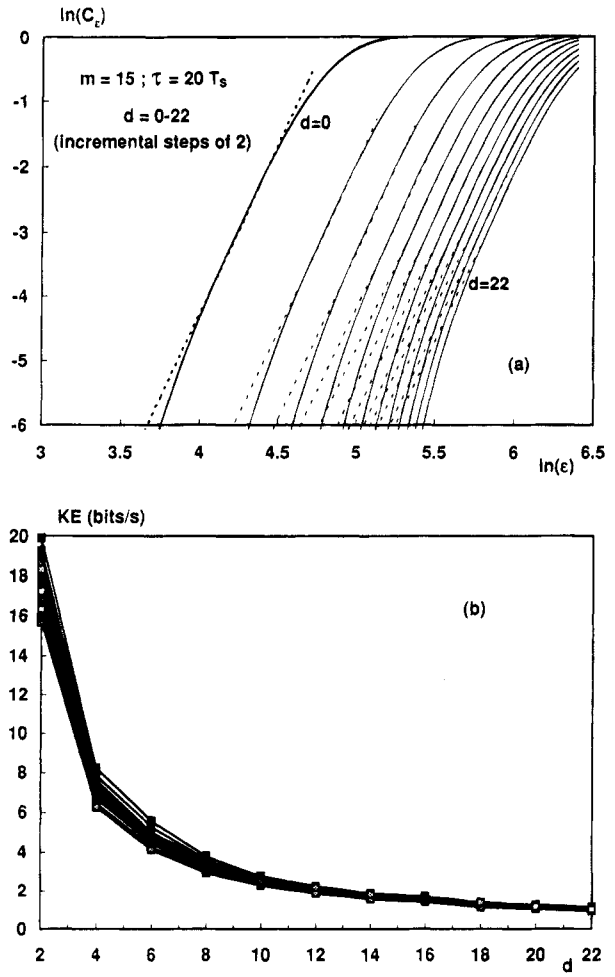

Figure 6. (a) Correlation integral for different numbers of consecutive points. (b) Convergence of the Kolmogorov entropy as "d" increases.

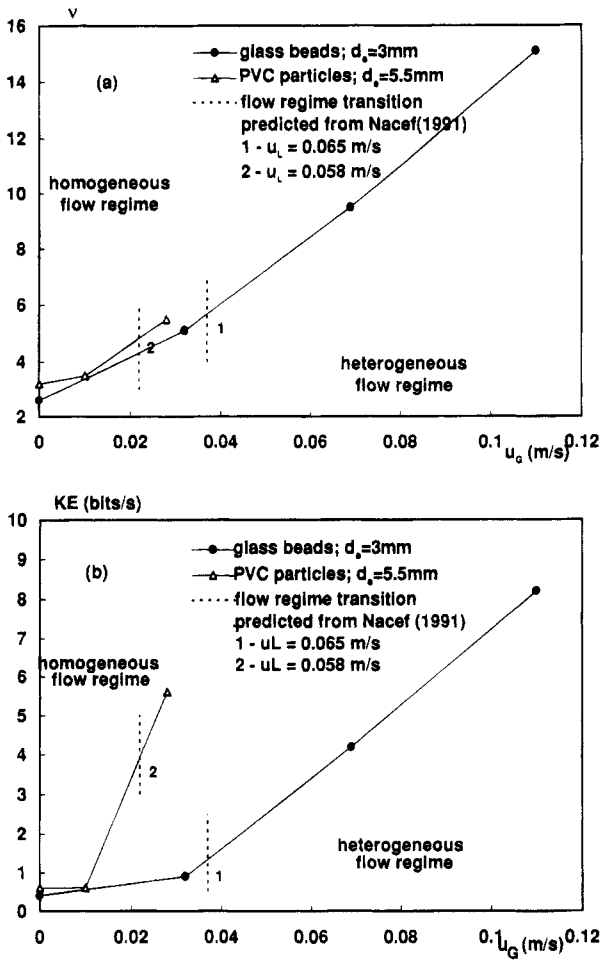

Figure 7. Effect of the gas superficial velocity on the estimated values of the (a) correlation dimensions and (b) Kolmogorov entropies. The dotted curve corresponds to the flow regime transition predicted by Nacef (1991).

break is observed in the trend for a change in flow regime. However, the Kolmogorov entropy tends to stay almost constant within the homogeneous flow regime and to increase with a steeper slope after the flow regime transition. Even if it is not included in the graphs, an experiment with a mixture of glass beads of 3 and 1 mm was also carried out at a gas superficial velocity of 0.11 m/s. The results are listed in Table 2. This experiment was clearly in the heterogeneous flow regime. The correlation dimension and the Kolmogorov entropy were of the order of magnitude of the corresponding values for the experiment with the 3 mm glass beads in the same flow regime. These results suggest that these parameters may characterize the flow regime and, consequently, their estimation may provide an objective quantitative way of determining flow regime transitions in a three-phase fluidized bed reactor.

It is likely that the chaotic characteristic of the solids motion is enhanced and closely linked to the presence of fast moving bubbles in the flow. This idea is reinforced by the high values of the Kolmogorov entropy observed in the bubbling flow regime in gas–solid fluidized beds (Schouten and van den Bleek, 1993b) compared to the relatively low values for circulating fluidized beds (Brouillard and Miller, 1993), liquid fluidized beds and three-phase fluidized beds in the homogeneous flow regime where the bubbles activity is less intense.

Conclusions

In this work, extended time series of positions of a solid tracer having the same properties as the particles constituting the fluidized bed are examined. A rescaled range analysis is employed to study the tracer fluctuating steps. The deterministic motion of the tracer is analyzed under the theory of deterministic chaos.

From the *R/S* analysis on the particle fluctuations, it is found that (1) solids turbulence is anisotropic in liquid–solid fluidization and for the homogeneous and heterogeneous regimes in three-phase fluidization. (2) In the horizontal, the solids fluctuating steps are not correlated; Hurst exponents are always around 0.5. Hence a Fickian law with a constant transverse dispersion coefficient correctly accounts for transverse dispersion in these systems. (3) For the axial coordinate, the fluctuating steps are always correlated. Therefore, a Fickian axial dispersion model cannot account for the solids axial dispersion in these systems. For three-phase fluidization and for liquid–solid fluidization in the particulate flow regime, the dispersion has superdispersive characteristics. For liquid–solid fluidization in the segregate regime there is subdispersion of the solids.

From the analysis of the solids motion according to deterministic chaos theory, it was found that (1) the solids dynamics in liquid–solid and three-phase fluidized beds is chaos as diagnosed by the positive values obtained for the Kolmogorov entropy. The degree of chaoticity increases as the gas superficial velocity is increased. As a chaotic behavior can only arise from nonlinear dynamics, mathematical models that aim at describing the solids motion in these systems should contain a minimum of nonlinear complexity. The strange attractor that characterizes these solids dynamics for liquid–solid fluidization and for three-phase fluidization with low gas velocities is of low dimension, indicating that the number of variables needed to describe the solids dynamics in a nonlinear frame is low for these cases. The attractor dimensions increase strongly with an increase in gas velocities. (2) A change in flow regime strongly affects the chaotic characteristics of the solid phase dynamics in three-phase fluidization. There is a strong change in the attractor shape and in the magnitude of the correlation dimension and the Kolmogorov entropy. Therefore, the estimation of these parameters appears as a promising objective tool for determining flow regime transitions in three-phase fluidized bed reactors.

Acknowledgment

The authors gratefully acknowledge financial support from the Natural Sciences and Engineering Research Council of Canada and the Fonds pour la Formation de Chercheurs et l'Aide à la Recherche (Québec). Collaboration of Dr. G. Kennedy for activation of the tracer and stimulating discussions with Dr. M. Grmela are also gratefully acknowledged.

Nomenclature

A = surface area (m^2)
c = cumulative departure from the mean for a FBM (m)
C = vector of the new basis of the state space obtained by SVD where the attractor is projected
C_ϵ = correlation integral
d_e = equivalent diameter (m)
d_p = particle diameter (m)
H = Hurst coefficient
KE = Kolmogorov entropy (bits/s)
m = embedding dimension
N = number of points in the attractor
R = sequential range (m)
s = time lag for the *R/S* analysis (time units)
S = variance of the fractional Brownian increments (m)
t = time (s)
t_0 = initial time for the *R/S* analysis (s)
T_s = sample period (s)
u = superficial velocity (m/s)
v = measured scalar variable (signal)
V = volume (m^3)
x = particle coordinate (m)
$\underline{x}_t$ = point of the attractor of which the initial coordinate is the measured variable at time "t"
X = position of the fractional Brownian particle (m)
y = particle coordinate (m)
z = particle coordinate (m)

Greek Letters

ϵ = radius of a chosen hypersphere in the embedding space
ϵ^* = radius of a chosen hypersphere in the embedding space, made dimensionless with the maximum size of the attractor
ν = correlation dimension
Θ = Heaviside function: $\Theta(x) = 1$ for $x < 0$ and 0 for $x > 0$
η = index to indicate the time in the *R/S* analysis (time units)
ϱ = density (kg/m^3)
τ = delay time (s)

Subscripts

G = gas
L = liquid
p = particle
S = solid

Superscripts

d = number of consecutive points to estimate the correlation integrals for KE calculation

Acronyms

FBM = Brownian motion
FBM = fractional Brownian motion
R/S = rescaled range
SVD = singular value decomposition

Literature Cited

Albano, A. M.; Muench, J.; Schwartz, C.; Mees, A. I.; Rapp, P. E. Singular-Value Decomposition and the Grassberger-Procaccia Algorithm. *Phys. Rev. A* **1988**, 38, 3017–3026.

Bickel, T. C.; Thomas, M. G. Catalyst Deactivation in the H-Coal Coal Liquefaction Process. 1. Catalyst Residence Time Distribution. *Ind. Eng. Chem. Process Des. Dev.* **1982**, *21*, 377–381.

van den Bleek, C. M.; Schouten, J. C. Can Deterministic Chaos Create Order in Fluidized-Bed Scale-Up? *Chem. Eng. Sci.* **1993a**, *48*, 2367–2373.

van den Bleek, C. M.; Schouten, J. C. Deterministic Chaos: a New Tool in Fluidized Bed Design and Operation. *Chem. Eng. J.* **1993b**, *53*, 75–87.

Bouillard, J.-X.; Miller, A. Experimental Investigation of Chaotic Hydrodynamic Attractors in Circulating Fluidized Beds. Abstract of Papers. 4th International Conference on Circulating Fluidized Beds, Pittsburgh, Pennsylvania, August 1–5, 1993.

Broomhead, D. S.; King, G. P. Extracting Qualitative Dynamics from Experimental Data. *Physica D* **1986**, *20*, 217–236.

Daw, C. S.; Halow, J. S. Characterization of Voidage and Pressure Signals from Fluidized Beds using Deterministic Chaos Theory. *Abstract of Papers*. 11th International Conference on Fluidized Bed Combustion; ASME: New York, 1991; Vol. 2.

Daw, C. S.; Halow, J. S. Modeling Deterministic Chaos in Gas Fluidized Beds. *AIChE Symp. Ser.* **1992**, *289*, 61–69.

Daw, C. S.; Lawkins, W. F.; Downing, D. J.; Clapp, N. E. Chaotic Characteristics of a Complex Gas-Solid Flow. *Phys. Rev. A* **1990**, *41*, 1179–1181.

Dudukoviĉ, M. P.; Devanathan, N.; Holub, R. Multiphase Reactors: Models and Experimental Verification. *Rev. Inst. Fr. Pet.* **1991**, *46*, 439–465.

Eckman, J. P.; Ruelle, D. Ergodic Theory of Chaos and Strange Attractors. *Rev. Mod. Phys.* **1985**, *57*, 617–656.

Euzen, J. P.; Fortin, Y. Partikelbewegung in einem Dreiphasenfliessbett. *Chem.-Ing.-Tech.* **1987**, *59*, 416–419.

Fan, L. S. *Gas-Liquid-Solid Fluidization Engineering*; Butterworths: Boston, 1989.

Fan, L. S.; Tzeng, J. W.; Bi, H. T. Flow Structure in a Two-Dimensional Bubble Column and Three-Phase Fluidized bed. In *Fluidization VII*; Engineering Foundation: New York, 1992; pp 399–406.

Farmer, J. D.; Ott, E.; Yorke, J. A. The Dimension of Chaotic Attractors. *Physica D* **1983**, *0*, 153–180.

Feder, J. *Fractals*; Plenum Press: New York, 1988.

Grassberger, P.; Procaccia, I. Measuring the Strangeness of Strange Attractors. *Physica D* **1983a**, *9*, 189–208.

Grassberger, P.; Procaccia, I. Estimation of the Kolmogorov Entropy from a Chaotic Signal. *Phys. Rev. A* **1983b**, *28*, 2591–2593.

Grassberger, P. Estimating the Fractal Dimensions and Entropies of Strange Attractors. In *Chaos*; Holden, A. V., Ed.; Princeton University Press: Princeton, NJ, 1986; Chapter 14, pp 291–311.

Khare, A. S.; Dharwadkar, S. V.; Joshi, J. B. Solid-Phase Mixing in Three-Phase Sparged Reactors. *J. Chem. Eng. Jpn.* **1989**, *22*, 125–130.

Hurst, H. E. Long-Term Storage Capacity of Reservoirs. *Trans. Am. Soc. Civ. Eng.* **1951**, *116*, 770–808.

Hilborn, R. C. *Chaos and Nonlinear Dynamics. An Introduction for Scientists and Engineers*; Oxford University Press: New York, 1994.

Larachi, F.; Chaouki, J.; Guy, C.; Kennedy, G. Solids Mixing Investigation in a Three-Phase Fluidized Bed. Presented at the 11th International Congress of Chemical Engineering, Chemical Equipment Design and Automation, Prague, Czech Republic; August 29–September 3, 1993; Session I1, Paper 560.

Larachi, F.; Kennedy, G.; Chaouki, J. A γ-Ray Detection System for 3-D Particle Tracking in Multiphase Reactors. *Nucl. Instrum. Methods Phys. Res., Sect. A* **1994**, *338*, 568–576.

Lin, J. S.; Chen, M. M.; Chao, B. T. A Novel Radioactive Particle Tracking Facility for Measurement of Solids Motion in Gas Fluidized Beds. *AIChE J.* **1985**, 31, 465–473.

Mandelbrot, B. B. *The Fractal Geometry of Nature*; W. H. Freeman and Company: New York, 1982.

Mandelbrot, B. B.; Van Ness, J. W. Fractional Brownian Motions, Fractional Noises and Applications. *SIAM Rev.* **1968**, *10*, 422–437.

Mandelbrot, B. B.; Wallis, J. R. Computer Experiments with Fractional Gaussian Noises. Part 2, Rescaled Ranges and Spectra. *Water Resour. Res.* **1969a**, *5*, 242–259.

Mandelbrot, B. B.; Wallis, J. R. Robustness of the Rescaled Range *R/S* in the Measurement of Noncyclic Long Run Statistical Dependence. *Water Resour. Res.* **1969b**, *5*, 967–988.

Moon, F. C. *Chaotic and Fractal Dynamics. An Introduction for Applied Scientists and Engineers*; John Wiley & Sons, Inc.: New York, 1992.

Moslemian, D.; Chen, M. M.; Chao, B. T. Experimental and Numerical Investigations of Solids Mixing in a Gas-Solid Fluidized Bed. *Part. Sci. Technol.* **1989**, *7*, 335–355.

Nacef, S. Hydrodynamique des Lits Fluidisés Gaz-Liquide-Solide. Effets du Distributeur et de la Nature du Liquide. Ph.D. Dissertation, Institut National Polytechnique de Lorraine, Nancy, France, 1991.

Ott, E. *Chaos in Dynamical Systems*; Cambridge University Press: New York, 1993.

Packard, N. H.; Crutchfield, J. P.; Farmer, J. D.; Shaw, R. S. Geometry from a Time Series. *Phys. Rev. Lett.* **1980**, *45*, 712–716.

Ruelle, D. *Chance and Chaos*; Princeton University Press: Princeton, NJ, 1991.

Stewart, I. *Does God Play Dice?. The Mathematics of Chaos*; Basil Blackwell Ltd.: Oxford, UK, 1989.

Stringer, J. Is a Fluidized Bed a Chaotic Dynamic System? *Abstract of Papers*. International Conference on Fluidized Bed Combustion (FBC) - Technology for Today, San Francisco, April 30-May 3, 1989; ASME: New York, 1989; Vol. 1.

Schouten, J. C.; van den Bleek, C. M. Chaotic Hydrodynamics of Fluidization: Consequences for Scaling and Modeling of Fluid Bed Reactors. *AIChE Symp. Ser.* **1992**, *289*, 70–84.

Takens, F. In *Lecture Notes in Mathematics*; Springer: New York, 1981; Vol. 898, p 366.

Theiler, J. Spurious Dimension from Correlation Algorithms Applied to Limited Times-Series Data. *Phys. Rev. A* **1986**, *34*, 2427–2432.

Theiler, J. Some Comments on the Correlation Dimension of $1/f^{\alpha}$ Noise. *Phys. Lett. A* **1991**, *155*, 480–493.

Tzeng, J. W.; Chen, R. C.; Fan, L. T. Visualization of Flow Characteristics in a 2-D Bubble Column and Three-Phase Fluidized Bed. *AIChE J.* **1993**, *39*, 733–744.

Wang, K. G.; Lung, C. W. Long Time Correlation Effects and Fractal Brownian Motion. *Phys. Lett.* **1990**, *151A*, 119–121.

Wild, G.; Poncin, S. Hydrodynamics. In *Three-phase Sparged Reactors*; Nigam, K. D. P., Schumpe, A., Eds.; Topics in Chem. Eng. Series Gordon & Breach Science Publishers: New York, 1994, Chapter 1, to appear.

Yang, Y. B.; Devanathan, N.; Dudukovič, M. P. Liquid Backmixing in Bubble Columns. *Chem. Eng. Sci.* **1992**, *47*, 2859–2864.

Received for review September 6, 1994
Revised manuscript received January 24, 1995
Accepted May 2, 1995[⊗]

IE940525Y

[⊗] Abstract published in *Advance ACS Abstracts,* June 15, 1995.